DISCRETE AND CONTINUOUS
DYNAMICAL SYSTEMS SERIES B
Volume **21**, Number **8**, October **2016**

doi:10.3934/dcdsb.2016054

pp. **2423–2449**

MODELING AND CONTROL OF LOCAL OUTBREAKS OF WEST NILE VIRUS IN THE UNITED STATES

Jing Chen

Department of Mathematics, University of Miami
Coral Gables, FL 33146, USA

Jicai Huang

School of Mathematics and Statistics, Central China Normal University
Wuhan 430079, China

John C. Beier

Department of Public Health Sciences
University of Miami Miller School of Medicine
Miami, FL 33136, USA

Robert Stephen Cantrell and Chris Cosner

Department of Mathematics, University of Miami
Coral Gables, FL 33146, USA

Douglas O. Fuller

Department of Geography and Regional Studies, University of Miami
Coral Gables, FL 33146, USA

Guoyan Zhang

Florida Department of Health, Miami-Dade County, Epidemiology
Disease Control and Immunizations Services
8600 NW 17th Street, Suite 200, Miami, FL 33126, USA

Shigui Ruan*

Department of Mathematics, University of Miami
Coral Gables, FL 33146, USA

(Communicated by Yuan Lou)

Abstract. West Nile virus (WNV) was first detected in the United States (U.S.) during an outbreak in New York City in 1999 with 62 human cases including seven deaths. In 2001, the first human case in Florida was identified, and in Texas and California it was 2002 and 2004, respectively. WNV has now been spread to almost all states in the US. In 2015, the Center for Disease Control and Prevention (CDC) reported 2,175 human cases, including

2010 *Mathematics Subject Classification.* Primary: 37N25, 92D25; Secondary: 92D30.

Key words and phrases. West Nile virus, mathematical modeling, basic reproduction number, sensitive analysis, transmission dynamics.

Research was partially supported by National Natural Science Foundation of China (No. 11471133), Self-determined Research Funds of CCNU from the Colleges' Basic Research and Operation of MOE (CCNU16A02009), National Science Foundation (DMS-1412454), and Convergence Research Groups grant of College of Arts and Sciences at the University of Miami.

* Corresponding author: Shigui Ruan (E-mail: ruan@math.miami.edu).

146 deaths, from 45 states. WNV is maintained in a cycle between mosquitoes and animal hosts in which birds are the predominant and preferred reservoirs while most mammals, including humans, are considered dead-end hosts, as they do not appear to develop high enough titers of WNV in the blood to infect mosquitoes. In this article, we propose a deterministic model by including interactions among mosquitoes, birds, and humans to study the local transmission dynamics of WNV. To validate the model, it is used to simulate the WNV human data of infected cases and accumulative deaths from 1999 to 2013 in the states of New York, Florida, Texas, and California as reported to the CDC. These simulations demonstrate that the epidemic of WNV in New York, Texas, and California (and thus in the U.S.) has not reached its equilibrium yet and may be expected to get worse if the current control strategies are not enhanced. Mathematical and numerical analyses of the model are carried out to understand the transmission dynamics of WNV and explore effective control measures for the local outbreaks of the disease. Our studies suggest that the larval mosquito control measure should be taken as early as possible in a season to control the mosquito population size and the adult mosquito control measure is necessary to prevent the transmission of WNV from mosquitoes to birds and humans.

1. **Introduction.** West Nile virus (WNV) is an emerging mosquito-borne RNA virus of global significance that can cause fatal neurological diseases by infecting the central nervous system of various host species (Hayes & Gubler [18]). It was first isolated from the blood of a febrile woman in the West Nile province of Uganda in 1937 and then was associated with the epidemics of febrile illness and sporadic encephalitis in Africa, the Mediterranean Basin, Europe, India, and Australia (DeBiase & Tyler [17]).

In the U.S., WNV was detected for the first time during an outbreak in New York City in 1999 (O'Leary et al. [30]; Murray et al. [28]), presumably after being introduced by migratory birds. It was first isolated from a dead American crow (Lanciotti et al. [21]) and then from carcasses of many other bird species collected between August and November 1999 (Anderson et al. [1]; Eidson et al. [15]; Steele et al. [35]). At the same time, WNV-specific RNA sequences were identified from fatal human cases (Briese et al. [5]; Lanciotti et al. [21]). After the initial outbreak in New York City in 1999, WNV continued to cause sporadic equine and human diseases in the U.S. (Marfin & Gubler [27]), and spread rapidly across North America and into Latin America and the Caribbean. In 2002, the largest outbreak of WNV encephalitis ever recorded occurred in the U.S., with numerous epicenters spread across the nation's mid-section, and virus activity occurring coast-to-coast, breaching both the Canadian and Mexican borders (Komar [20]). In Florida (Blackmore et al. [3]), Texas (Nolan et al. [29]), and California (Reisen et al. [32]), the first human cases were reported in 2001, 2002, and 2004, respectively. The data reported by CDC indicates that, from 1999 to 2013, there were 39,557 cases including 1,668 deaths from 49 states in the U.S. (CDC [7]).

WNV is maintained in a cycle between mosquitoes and animal hosts, in which birds are the predominant and preferred reservoirs (Anderson et al. [1]). Bird infection is most often the result of bites from infected mosquitoes. After being bitten by infected mosquitoes, some species of birds show symptoms of disease and may die, while others serve as reservoirs without showing signs of disease. Crows and house sparrows are highly susceptible to WNV, but the American robin is thought to be the main host species for the maintenance and transmission of WNV in the U.S, since it is preferred by the dominant mosquito species *Culex pipiens* (Hamer et al. [16]; Kilpatrick et al. [19]).

Mosquitoes become infected when they feed on infected birds. When the blood meal is being digested, the virus infects and replicates in the midgut epithelia cells of the mosquito. After replicating, the virus travels through the mosquito hemolymph to the salivary glands and accumulates in the salivary glands (Colpitts et al. [9]). During later blood meals, the virus may be injected into humans and animals. The incubation period usually lasts from 3 to 14 days. Most people (about 80%) who become infected with WNV do not develop any symptoms. For other infected people, the virus will result in a mild febrile illness whose symptoms include a fever with other symptoms such as headache, body aches, joint pains, vomiting, diarrhea, or rash. Less than 1% of those infected people will develop neuroinvasive diseases such as encephalitis or meningitis or West Nile poliomyelitis (CDC [7]).

Though WNV has been studied extensively in the last decade, considering the absence of a specific treatment and vaccine for WNV, further research is needed to understand the epidemiology and pathology of WNV as an underlying persistent infection.

Various mathematical models have been proposed to describe the transmission dynamics of WNV. Thomas & Urena [36] used a difference equation model involving birds, mosquitoes, and humans to investigate the effectiveness of pesticide spraying to reduce mosquito populations and in succession human WNV encephalitis in New York City after the outbreak in 1999. Wonham et al. [40] proposed a deterministic SIR model of WNV cross-infection between birds and mosquitoes, derived the basic reproduction number $\mathcal{R}_0$, provided a method for determining necessary mosquito control levels, and provided numerical simulations that are consistent with mosquito and bird data. Cruz-Pacheco et al. [12] presented a similar WNV model and numerical results to incorporate the influence of mosquito vertical transmission on WNV dynamics and estimated $\mathcal{R}_0$ values for eight common bird species. Bowman et al. [4] extended the mosquito-bird transmission cycle to five compartments for humans including hospitalization of WNV patients, calculated $\mathcal{R}_0$, determined the stability of the disease-free and endemic equilibria by using $\mathcal{R}_0$ as a threshold, and accessed the two main WNV prevention strategies: mosquito reduction and personal protection. Laperriere et al. [22] developed an epidemic model with environmental temperature for the simulation of the WNV dynamics of mosquitoes, birds, horses and humans and applied it to simulate the monthly WNV data of reported bird, equine, and human cases in the Minneapolis metropolitan area (Minnesota). Wan and Zhu [39] discussed the backward bifurcation in compartmental WNV models. Simpson et al. [34] developed an empirically informed transmission model for WNV in four sites using one vector species (*Cx. pipiens*) and preferred and non-preferred avian hosts and found that host preference-induced contact heterogeneity is a key mediator of vector-borne pathogen epizootics in multi-species host communities. For a survey on the comparison of some of these models, we refer to Wonham et al. [41]. However, most of these models focus on the transmission dynamics between the birds and mosquitoes. There are very few studies (Thomas & Urena [36], Bowman et al. [4], Laperriere et al. [22]) on modeling the interaction among mosquitoes, birds and humans whereas the existing data from the CDC are mainly human cases. Moreover, there has been very little research (Laperriere et al. [22]) on simulating reported WNV human data. Furthermore, it is known that mosquito control is one of the main prevention strategies, but how mosquito (larval and adult) control measures affect the prevalence of the disease at the human level has not been studied and is not well-understood.

In this paper, we propose a mathematical model to study the transmission dynamics of WNV by taking into account the local interactions between birds and mosquitoes as well as the transmission from mosquitoes to human. Based on this model, we discuss the existence of the disease-free and endemic equilibria. To validate the model, we use the model to simulate the WNV human data of infected cases and accumulative deaths from 1999 to 2013 in the states of New York, Florida, Texas, and California, which were reported by the CDC. Then we study the basic properties of the model, including the boundedness of solutions, existence and stability of the disease-free equilibrium, existence of the endemic equilibrium, and existence of backward bifurcation. We also give some reasonable predictions for these four states for the coming years. Finally, by carrying out sensitivity analysis of the basic reproduction number $\mathcal{R}_0$ in terms of model parameters, we try to explore some strategies to prevent and control the local outbreaks of WNV.

2. **Model formulation.** In this section, we present a mathematical model to study the transmission dynamics of WNV. The model is based on a susceptible, exposed, infectious, and recovered (SEIR) structure and explains the transmission process among humans, birds and mosquitoes.

Let $S_M(t)$, $E_M(t)$ and $I_M(t)$ denote the number of susceptible, exposed, and infectious mosquitoes at time t, respectively. Similarly, $S_B(t)$, $E_B(t)$, $I_B(t)$, $R_B(t)$, $S_H(t)$, $E_H(t)$, $I_H(t)$, and $R_H(t)$ represent the number of susceptible, exposed, infectious, and recovered birds/humans at time t. Here the total mosquito population is denoted by $N_M(t) = S_M(t) + E_M(t) + I_M(t)$. Meanwhile, $N_B(t) = S_B(t) + E_B(t) + I_B(t) + R_B(t)$ and $N_H(t) = S_H(t) + E_H(t) + I_H(t) + R_H(t)$ are the total numbers of birds and humans. Our assumptions are given in the flowchart (Fig 1)

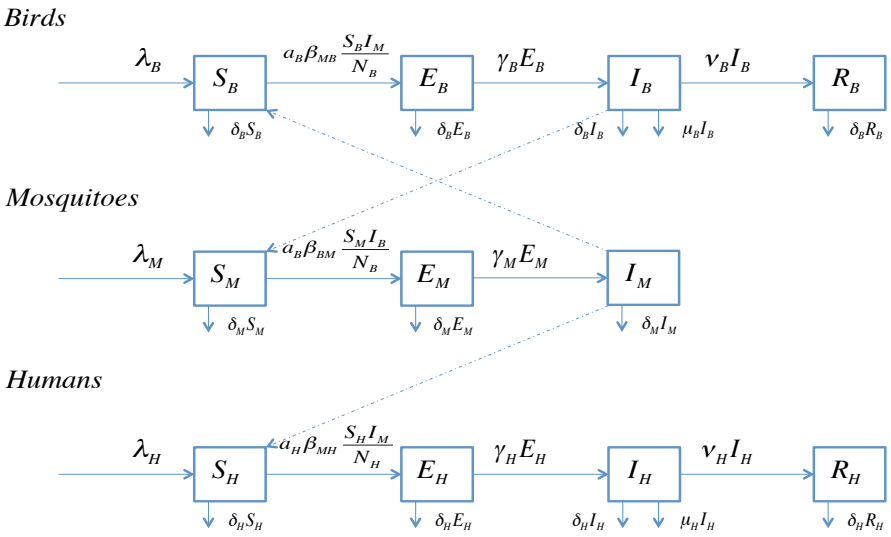

FIGURE 1. Flowchart of the West Nile virus model.

When a mosquito is infected by WNV, a susceptible person or bird may be infected through bites of this infectious mosquito. The cross-infection between birds

or humans and mosquitoes is modeled as $a_B\beta_{MB}\frac{S_BI_M}{N_B}$ or $a_H\beta_{MH}\frac{S_HI_M}{N_H}$ by the frequency-dependent biting assumption of mosquitoes, where a_B and a_H describe per capita biting rate of mosquitoes on birds and humans, respectively. The probabilities of WNV transmission from mosquitoes to birds and humans are denoted by β_{MB} and β_{MH}, respectively. Similarly, the infection of mosquitoes through biting the infectious birds is described by $a_B\beta_{BM}\frac{S_MI_B}{N_B}$, where β_{BM} is the probability of WNV transmission from birds to mosquitoes.

For other parameters, those $\lambda's$ with the subscripts B, M and H refer to the recruitment rates of birds, mosquitoes and humans, respectively. γ $(\gamma_M, \gamma_B, \gamma_H)$ refers to the rate moving from the exposed class to the infectious class. The parameters labelled ν (ν_B, ν_H) describe the recovery rate and those labelled μ (μ_B, μ_H) represent the WNV-induced death rate, respectively. All those labelled δ $(\delta_M, \delta_B, \gamma_H)$ are defined as the natural death rate of birds, mosquitoes and humans, respectively.

Based on the assumptions and the flowchart, our model is consisted of the following equations:

$$\begin{aligned}
\frac{dS_M}{dt} &= \lambda_M - a_B\beta_{BM}\frac{S_MI_B}{N_B} - \delta_MS_M\\
\frac{dE_M}{dt} &= a_B\beta_{BM}\frac{S_MI_B}{N_B} - \delta_ME_M - \gamma_ME_M\\
\frac{dI_M}{dt} &= \gamma_ME_M - \delta_MI_M\\
\frac{dS_B}{dt} &= \lambda_B - a_B\beta_{MB}\frac{S_BI_M}{N_B} - \delta_BS_B\\
\frac{dE_B}{dt} &= a_B\beta_{MB}\frac{S_BI_M}{N_B} - \delta_BE_B - \gamma_BE_B\\
\frac{dI_B}{dt} &= \gamma_BE_B - \delta_BI_B - \mu_BI_B - \nu_BI_B\\
\frac{dR_B}{dt} &= \nu_BI_B - \delta_BR_B\\
\frac{dS_H}{dt} &= \lambda_H - a_H\beta_{MH}\frac{S_HI_M}{N_H} - \delta_HS_H\\
\frac{dE_H}{dt} &= a_H\beta_{MH}\frac{S_HI_M}{N_H} - \delta_HE_H - \gamma_HE_H\\
\frac{dI_H}{dt} &= \gamma_HE_H - \delta_HI_H - \mu_HI_H - \nu_HI_H\\
\frac{dR_H}{dt} &= \nu_HI_H - \delta_HR_H.
\end{aligned} \tag{1}$$

All parameters are nonnegative constants with their biological interpretations given in Table 1.

Specific parameter values will be given in section 4 when the model is used to fit the reported WNV data from New York, Florida, Texas and California. Notice that the WNV data reported by CDC are annual data (and the reported incidence rates and disease-induced rates are annual rates as well). In order to use model (1) to simulate the annual WNV data from CDC, we use a percentage per year to describe some parameters so that the time unit is year. For example, $\gamma_H = 20\%/year$ means that annually 20% of exposed humans will progress to the infectious class.

3. **Mathematical analysis.**

3.1. **Basic properties.**

Using standard analysis we can show that all solutions to system (1) are nonnegative. We can also see that the total population of mosquitoes

TABLE 1. Parameters of model (1) and their interpretations.

Parameter	Description	Values
λ_B	Recruitment rate of susceptible birds	Estimated
λ_M	Recruitment rate of susceptible mosquitoes	Estimated
λ_H	Recruitment rate of susceptible humans	Fixed [37]
δ_B	Death rate of birds	Fixed [10]
δ_M	Death rate of mosquitoes	Estimated
δ_H	Natural death rate of humans	Fixed [37]
γ_B	Progression rate of birds from exposed to infectious	Estimated
γ_M	Progression rate of mosquitoes from exposed to infectious	Estimated
γ_H	Progression rate of humans from exposed to infectious	20% [42]
μ_B	Disease-induced death rate of birds	Estimated
μ_H	Disease-induced death rate of humans	Fixed (Table 3)
ν_B	Recovery rate of birds	Estimated
ν_H	Recovery rate of humans	Estimated
a_B	Per capita biting rate of mosquitoes on birds	0.03-0.16 [40]
a_H	Per capita biting rate of mosquitoes on humans	0.03-0.16 [40]
β_{BM}	Probability of transmission from birds to mosquitoes	16% [33]
β_{MB}	Probability of transmission from mosquitoes to birds	88% [40]
β_{MH}	Probability of transmission from mosquitoes to humans	0-1

satisfies the differential equation

$$\frac{dN_M}{dt} = \lambda_M - \delta_M N_M. \tag{2}$$

This implies that $N_M(t) \to \frac{\lambda_M}{\delta_M}$ as $t \to +\infty$, so the limiting set of system (1) is on the plane $S_M + E_M + I_M = \frac{\lambda_M}{\delta_M}$. Similarly we can obtain

$$\begin{aligned} \frac{dN_B}{dt} &= \lambda_B - \delta_B N_B - \mu_B I_B \\ \frac{dN_H}{dt} &= \lambda_H - \delta_H N_H - \mu_H I_H. \end{aligned} \tag{3}$$

These lead to

$$\begin{aligned} \lambda_B - (\delta_B + \mu_B) N_B \le \frac{dN_B}{dt} \le \lambda_B - \delta_B N_B, \\ \lambda_H - (\delta_H + \mu_H) N_H \le \frac{dN_H}{dt} \le \lambda_H - \delta_H N_H. \end{aligned} \tag{4}$$

Each of the total subpopulations $N_M(t)$, $N_B(t)$ and $N_H(t)$ is assumed to be positive for $t = 0$. Following (4), all solutions of system (1) remain nonnegative and

$$\begin{aligned} \Lambda = \{(E_M, I_M, S_B, E_B, I_B, R_B) \mid 0 \le E_M + I_M \le \frac{\lambda_M}{\delta_M}, \frac{\lambda_B}{\delta_B + \mu_B} \le S_B + E_B \\ + I_B + R_B \le \frac{\lambda_B}{\delta_B}, \frac{\lambda_H}{\delta_H + \mu_H} \le S_H + E_H + I_H + R_H \le \frac{\lambda_H}{\delta_H}\}. \end{aligned}$$

is positively invariant for system (1).

3.2. **Disease-free equilibrium and the basic reproduction number.** Model (1) has a disease-free equilibrium (DFE), obtained by setting the right hand sides of (1) to zero, given by

$$E_0 = \left(\frac{\lambda_M}{\delta_M}, 0, 0, \frac{\lambda_B}{\delta_B}, 0, 0, 0, \frac{\lambda_H}{\delta_H}, 0, 0, 0\right).$$

Following Diekman et al. [13, 14] and van den Driessche and Watmough [38], we have

$$F = \begin{pmatrix} 0 & 0 & 0 & \frac{a_B\beta_{BM}\lambda_M\delta_B}{\delta_M\lambda_B} & 0 & 0 \\ 0 & 0 & 0 & 0 & 0 & 0 \\ 0 & a_B\beta_{MB} & 0 & 0 & 0 & \\ 0 & 0 & 0 & 0 & 0 & 0 \\ 0 & a_H\beta_{MH} & 0 & 0 & 0 & \\ 0 & 0 & 0 & 0 & 0 & \end{pmatrix},$$

$$V = \begin{pmatrix} \delta_M+\gamma_M & 0 & 0 & 0 & 0 & \\ -\gamma_M & \delta_M & 0 & 0 & 0 & 0 \\ 0 & 0 & \delta_B+\gamma_B & 0 & 0 & 0 \\ 0 & 0 & -\gamma_B & \delta_B+\mu_B+\nu_B & 0 & 0 \\ 0 & 0 & 0 & 0 & \delta_H+\gamma_H & 0 \\ 0 & 0 & 0 & 0 & -\gamma_H & \delta_H+\mu_H+\nu_H \end{pmatrix}.$$

The basic reproduction number $\mathcal{R}_0$ is defined to be the spectral radius (dominant eigenvalue) of the non-negative matrix FV^{-1}, denoted by $\rho(FV^{-1})$. Thus,

$$\mathcal{R}_0 = \rho(FV^{-1}) = \sqrt{\frac{a_B^2\gamma_B\gamma_M\beta_{BM}\beta_{MB}\lambda_M\delta_B}{\delta_M^2\lambda_B(\delta_M+\gamma_M)(\delta_B+\gamma_B)(\delta_B+\mu_B+\nu_B)}}. \tag{5}$$

In fact, every infectious bird averagely produces $a_B\frac{\lambda_M}{\delta_M}\frac{\delta_B}{\lambda_B}\beta_{BM}\frac{\gamma_M}{\delta_M(\delta_M+\gamma_M)}$ new infectious mosquitoes and each infectious mosquito produces $a_B\beta_{MB}\frac{\gamma_B}{(\delta_B+\gamma_B)(\delta_B+\mu_B+\nu_B)}$ new infectious birds over its infectious period. Thus the basic reproduction number, which is the number of new infections in the next generation of birds caused by one infectious bird through a generation of infections in mosquitoes, is given as

$$\sqrt{\frac{a_B^2\gamma_B\gamma_M\beta_{BM}\beta_{MB}\lambda_M\delta_B}{\delta_M^2\lambda_B(\delta_M+\gamma_M)(\delta_B+\gamma_B)(\delta_B+\mu_B+\nu_B)}}.$$

Theorem 2 of van den Driessche and Watmough [38] implies the following local stability result about E_0.

Theorem 3.1. *For system (1), the disease-free equilibrium E_0 is locally asymptotically stable if $\mathcal{R}_0 < 1$ and unstable if $\mathcal{R}_0 > 1$.*

3.3. **Endemic equilibrium of the reduced subsystem.** Let

$$E^* = (S_M^*, E_M^*, I_M^*, S_B^*, E_B^*, I_B^*, R_B^*, S_H^*, E_H^*, I_H^*, R_H^*)$$

be an arbitrary equilibrium of model (1) and denote

$$N_H^* = S_H^* + E_H^* + I_H^* + R_H^*.$$

Then the Jacobian matrix of the vector field corresponding to system (1), evaluated at E^*, is

$$J(E^*) = \begin{pmatrix} A_{11} & 0 \\ A_{21} & A_{22} \end{pmatrix},$$

where A_{11} will be given later and A_{22} is given by

$$\begin{pmatrix} -\frac{a_H\beta_{MH}I_M^*(N_H^*-S_H^*)}{(N_H^*)^2}-\delta_H & \frac{a_H\beta_{MH}I_M^*S_H^*}{(N_H^*)^2} & \frac{a_H\beta_{MH}I_M^*S_H^*}{(N_H^*)^2} & \frac{a_H\beta_{MH}I_M^*S_H^*}{(N_H^*)^2} \\ -\frac{a_H\beta_{MH}I_M^*(N_H^*-S_H^*)}{(N_H^*)^2} & -\frac{a_H\beta_{MH}I_M^*S_H^*}{(N_H^*)^2}-\delta_H-\gamma_H & -\frac{a_H\beta_{MH}I_M^*S_H^*}{(N_H^*)^2} & -\frac{a_H\beta_{MH}I_M^*S_H^*}{(N_H^*)^2} \\ 0 & \gamma_H & -(\delta_H+\mu_H+\nu_H) & 0 \\ 0 & 0 & \nu_H & -\delta_H \end{pmatrix}.$$

After extensive algebraic calculations by using the software *Mathematica*, the characteristic equation associated with A_{22} is given by

$$(\lambda+\delta_H)(\lambda^3+b_2\lambda^2+b_1\lambda+b_0)=0,$$

where

$$b_2=\frac{a_H\beta_{MH}I_M^*}{N_H^*}+\gamma_H+3\delta_H+\mu_H+\nu_H,$$

$$b_1=\gamma_H(2\delta_H+\mu_H+\nu_H)+\delta_H(3\delta_H+2(\mu_H+\nu_H))+\frac{a_H\beta_{MH}I_M^*(\gamma_H+2\delta_H+\mu_H+\nu_H)}{N_H^*},$$

$$b_0=\delta_H(\gamma_H+\delta_H)(\delta_H+\mu_H+\nu_H)+\frac{a_H\beta_{MH}I_M^*(N_H^*(\gamma_H+\delta_H)(\delta_H+\mu_H+\nu_H)-S_H^*\gamma_H\mu_H)}{(N_H^*)^2}.$$

It is easy to see that $b_2>0$ and $b_0>0$ because $N_H^*\geq S_H^*$. After some algebraic calculations, we also obtain that

$$\begin{aligned}b_2b_1-b_0 &= \frac{1}{(N_H^*)^2}[(\gamma_H+2\delta_H+\mu_H+\nu_H)((I_M^*a_H\beta_{MH})^2\\ &\quad+(N_H^*)^2(\gamma_H+2\delta_H)(2\delta_H+\mu_H+\nu_H))+I_M^*a_H\beta_{MH}(S_H^*\gamma_H\mu_H\\ &\quad+N_H^*(\gamma_H+2\delta_H+\mu_H+\nu_H)(\gamma_H+4\delta_H+\mu_H+\nu_H))]>0.\end{aligned}$$

So the Routh-Hurwitz criteria show that all eigenvalues of the matrix A_{22} have negative real parts. Thus the stability of the equilibrium E^* is determined by the eigenvalues of the matrix A_{11}, which is also the Jacobian matrix of the first seven equations of system (1) evaluated at E^*. Hence, the following seven-dimensional subsystem of (1),

$$\begin{aligned}\frac{dS_M}{dt}&=\lambda_M-a_B\beta_{BM}\frac{S_MI_B}{N_B}-\delta_MS_M\\ \frac{dE_M}{dt}&=a_B\beta_{BM}\frac{S_MI_B}{N_B}-\delta_ME_M-\gamma_ME_M\\ \frac{dI_M}{dt}&=\gamma_ME_M-\delta_MI_M\\ \frac{dS_B}{dt}&=\lambda_B-a_B\beta_{MB}\frac{S_BI_M}{N_B}-\delta_BS_B\\ \frac{dE_B}{dt}&=a_B\beta_{MB}\frac{S_BI_M}{N_B}-\delta_BE_B-\gamma_BE_B\\ \frac{dI_B}{dt}&=\gamma_BE_B-\delta_BI_B-\mu_BI_B-\nu_BI_B\\ \frac{dR_B}{dt}&=\nu_BI_B-\delta_BR_B,\end{aligned}\tag{6}$$

which describes the primary transmission cycle between mosquitoes and birds, determines the stability of any arbitrary equilibrium of the whole system (1). This can also be observed by noticing that none of the parameters about humans appears in the formula for basic reproduction number as a result of the fact that humans are the dead-end hosts of WNV.

To discuss the existence of an endemic equilibrium of (6), we set

$$D(I_B)=a_2I_B^2+a_1I_B+a_0=0,\tag{7}$$

where

$$\begin{aligned}a_2&=(\gamma_B+\delta_B)(\delta_B+\mu_B+\nu_B)(\gamma_M+\delta_M)\delta_M\mu_B(\delta_M\mu_B-a_B\beta_{BM}\delta_B),\\ a_1&=(\gamma_B+\delta_B)(\delta_B+\mu_B+\nu_B)[\lambda_B\delta_M(\gamma_M+\delta_M)(a_B\beta_{BM}\delta_B-2\delta_M\mu_B)\\ &\quad+a_B^2\beta_{BM}\beta_{MB}\gamma_M\lambda_M\delta_B],\\ a_0&=\lambda_B^2\delta_M^2(\gamma_B+\delta_B)(\gamma_M+\delta_M)(1-\mathcal{R}_0^2),\end{aligned}\tag{8}$$

and denote

$$\Delta = a_1^2 - 4a_2a_0, \quad I_B^{**} = \frac{\gamma_B\lambda_B}{(\gamma_B+\delta_B)(\delta_B+\mu_B+\nu_B)}.$$

Now we state the results on the existence of equilibria of system (6).

Theorem 3.2. *System (6) can have up to two endemic equilibria which are classified as follows.*

(i) The disease-free equilibrium (DFE) (i.e, the boundary equilibrium) $E_0(\frac{\lambda_M}{\delta_M}, 0, 0, \frac{\lambda_B}{\delta_B}, 0, 0, 0)$*, always exists.*

(ii) If $\mathcal{R}_0 < 1$ *and*

(a) $a_2 \le 0$*, then there is no positive equilibrium;*

(b) $a_2 > 0$*, then system (6) has two positive equilibria* $E^1(S_M^1, E_M^1, I_M^1, S_B^1, E_B^1, I_B^1, R_B^1)$ *and* $E^2(S_M^2, E_M^2, I_M^2, S_B^2, E_B^2, I_B^2, R_B^2)$ *if and only if*

$$\Delta > 0 \quad \text{and} \quad 0 < \frac{-a_1}{2a_2} < I_B^{**}, \tag{9}$$

where $I_B^1 = \frac{-a_1-\sqrt{\Delta}}{2a_2}$, $I_B^2 = \frac{-a_1+\sqrt{\Delta}}{2a_2}$, *and for* $i = 1, 2$

$$\begin{aligned}
S_M^i &= \frac{\lambda_M}{\delta_M} + \frac{a_B\beta_{BM}\delta_B\lambda_M I_B^i}{\delta_M(I_B^*(\delta_M\mu_B - a_B\beta_{BM}\delta_B) - \delta_M\lambda_B)},\\
E_M^i &= -\frac{a_B\beta_{BM}\delta_B\lambda_M I_B^i}{(\gamma_M+\delta_M)(I_B^i(\delta_M\mu_B - a_B\beta_{BM}\delta_B) - \delta_M\lambda_B)},\\
I_M^i &= -\frac{a_B\beta_{BM}\gamma_M\delta_B\lambda_M I_B^i}{\delta_M(\gamma_M+\delta_M)(I_B^i(\delta_M\mu_B - a_B\beta_{BM}\delta_B) - \delta_M\lambda_B)},\\
S_B^i &= \frac{\gamma_B\lambda_B - (\gamma_B+\delta_B)(\delta_B+\mu_B+\nu_B)I_B^i}{\gamma_B\delta_B},\\
E_B^i &= \frac{(\delta_B+\mu_B+\nu_B)I_B^i}{\gamma_B}, \quad R_B^i = \frac{\nu_B I_B^i}{\delta_B}.
\end{aligned}$$

Moreover, these two positive equilibria coalesce when $\Delta = 0$.

(iii) If $\mathcal{R}_0 > 1$*, then system (6) has one positive equilibrium* $E^*(S_M^*, E_M^*, I_M^*, S_B^*, E_B^*, I_B^*, R_B^*)$*, where*

$$\begin{aligned}
S_M^* &= \frac{\lambda_M}{\delta_M} + \frac{a_B\beta_{BM}\delta_B\lambda_M I_B^*}{\delta_M(I_B^*(\delta_M\mu_B - a_B\beta_{BM}\delta_B) - \delta_M\lambda_B)},\\
E_M^* &= -\frac{a_B\beta_{BM}\delta_B\lambda_M I_B^*}{(\gamma_M+\delta_M)(I_B^*(\delta_M\mu_B - a_B\beta_{BM}\delta_B) - \delta_M\lambda_B)},\\
I_M^* &= -\frac{a_B\beta_{BM}\gamma_M\delta_B\lambda_M I_B^*}{\delta_M(\gamma_M+\delta_M)(I_B^*(\delta_M\mu_B - a_B\beta_{BM}\delta_B) - \delta_M\lambda_B)},\\
S_B^* &= \frac{\gamma_B\lambda_B - (\gamma_B+\delta_B)(\delta_B+\mu_B+\nu_B)I_B^*}{\gamma_B\delta_B},\\
E_B^* &= \frac{(\delta_B+\mu_B+\nu_B)I_B^*}{\gamma_B}, \quad R_B^* = \frac{\nu_B I_B^*}{\delta_B},
\end{aligned}$$

and $I_B^* = \frac{-a_0}{a_1}$ *if* $a_2 = 0$; $I_B^* = \frac{-a_0+\sqrt{\Delta}}{2a_2}$ *if* $a_2 > 0$; *and* $I_B^* = \frac{-a_0-\sqrt{\Delta}}{2a_2}$ *if* $a_2 < 0$.

Proof. It is obvious that the disease-free equilibrium $E_0(\frac{\lambda_M}{\delta_M}, 0, 0, \frac{\lambda_B}{\delta_B}, 0, 0, 0)$ always exists and is unique. Now we prove the other two cases. Notice that $N_M = S_M +$

$E_M + I_M = \frac{\lambda_M}{\delta_M}$. We can see that a positive equilibrium of (6) must satisfy the following equations:

$$\begin{aligned}
&a_B\beta_{BM}\frac{(\frac{\lambda_M}{\delta_M} - E_M - I_M)I_B}{N_B} - \delta_M E_M - \gamma_M E_M = 0,\\
&\gamma_M E_M - \delta_M I_M = 0,\\
&\lambda_B - a_B\beta_{MB}\frac{S_B I_M}{N_B} - \delta_B S_B = 0,\\
&a_B\beta_{MB}\frac{S_B I_M}{N_B} - \delta_B E_B - \gamma_B E_B = 0,\\
&\gamma_B E_B - \delta_B I_B - \mu_B I_B - \nu_B I_B = 0,\\
&\nu_B I_B - \delta_B R_B = 0.
\end{aligned} \tag{10}$$

From the last four equations of (10), we can express S_B, E_B, and R_B in terms of I_B, respectively. When plugging these into the first and second equations, both E_M and I_M can be written in terms of I_B. Thus, we have

$$\begin{aligned}
E_M &= -\frac{a_B\beta_{BM}\delta_B\lambda_M I_B}{(\gamma_M+\delta_M)(I_B(\delta - M\mu_B - a_B\beta_{BM}\delta_B))},\\
I_M &= -\frac{a_B\beta_{BM}\gamma_M\delta_B\lambda_M I_B}{\delta_M(\gamma_M+\delta_M)(I_B(\delta_M\mu_B - a_B\beta_{BM}\delta_B) - \delta_M\lambda_B)},\\
S_B &= \frac{\gamma_B\lambda_B - (\gamma_B+\delta_B)(\delta_B+\mu_B+\nu_B)I_B}{\gamma_B\delta_B},\\
E_B &= \frac{(\delta_B+\mu_B+\nu_B)I_B}{\gamma_B},\quad R_B = \frac{\nu_B I_B}{\delta_B}.
\end{aligned} \tag{11}$$

Since $S_B > 0$, we have $I_B < I_B^{**} = \frac{\gamma_B\lambda_B}{(\gamma_B+\delta_B)(\delta_B+\mu_B+\nu_B)}$. Substituting (11) into the third equation of (10) gives a quadratic equation of I_B and the existence of endemic equilibrium depends on the number of roots of this equation in the interval $(0, I_B^{**})$. Substituting $I_B = I_B^{**} = \frac{\gamma_B\lambda_B}{(\gamma_B+\delta_B)(\delta_B+\mu_B+\nu_B)}$ into $f(I_B)$ gives

$$\begin{aligned}
D(I_B^{**}) = \frac{\delta_M\lambda_B^2(\gamma_M+\delta_M)(\gamma_B(\delta_B+\nu_B)+\delta_B(\delta_B+\mu_B+\nu_B))}{(\gamma_B+\delta_B)(\delta_B+\mu_B+\nu_B)}(a_B\beta_{BM}\gamma_B\delta_B\\
+\delta_M\nu_B\gamma_B + \delta_B\delta_M(\delta_B\delta_M(\delta_B+\gamma_B+\mu_B+\nu_B))) > 0.
\end{aligned}$$

If $\mathcal{R}_0 < 1$, then $a_0 > 0$. This implies that $f(0) > 0$ and $f(I_B^{**}) > 0$. When $a_2 \le 0$, there is no root in the interval $[0, I_B^{**}]$. When $a_2 > 0$, the characteristic equation (7) has two distinct roots if and only if $\Delta > 0$ and $0 < \frac{-a_1}{2a_2} < I_B^{**}$. Moreover, these two become one root with multiplicity two in the case of $\Delta = 0$.

If $\mathcal{R}_0 > 1$, then $a_0 < 0$. In fact $f(0) < 0$ and $f(I_B^{**}) > 0$ guarantee that the quadratic equation (7) has just one root in the interval $(0, I_B^{**})$. When $a_2 > 0$, this root is $\frac{-a_0+\sqrt{\Delta}}{2a_2}$; when $a_2 < 0$, it is $\frac{-a_0-\sqrt{\Delta}}{2a_2}$; and it is $\frac{-a_0}{a_1}$ when a_2 is zero. □

3.4. **Backward bifurcation.** From Theorem 3.3, we know that system (6) has multiple endemic equilibria if and only if

$$\mathcal{R}_0 < 1, \quad a_2 > 0, \quad \Delta > 0 \quad \text{and} \quad 0 < \frac{-a_1}{2a_2} < I_B^{**}. \tag{12}$$

First, we choose δ_M and λ_M as parameters and $\mathcal{R}_0 = 1$ defines a curve. Let C_0 be this cubic curve in the first quadrant:

$$C_0 : \lambda_M = \frac{\lambda_B(\gamma_B+\delta_B)(\delta_B+\mu_B+\nu_B)}{a_B^2\beta_{MB}\beta_{BM}\gamma_B\gamma_M\delta_B}\delta_M^2(\delta_M+\gamma_M), \quad \delta_M > 0.$$

For $a_2 > 0$, δ_M is required to be greater than $\frac{a_B\beta_{BM}\delta_B}{\mu_B}$. We denote the curve defined by $a_1 = 0$ as C_1 and the one defined by $\frac{-a_1}{2a_2} = I_B^{**}$ as C_{12}. Here, we let $K = \gamma_B(\delta_B - \mu_B + \nu_B) + \delta_B(\delta_B + \mu_B + \nu_B)$. Then

$$C_1 : \lambda_M = \frac{2\mu_B\lambda_B}{a_B^2\beta_{MB}\beta_{BM}\gamma_M\delta_B}\delta_M(\delta_M + \gamma_M)(\delta_M - \frac{a_B\beta_{BM}\delta_B}{2\mu_B}), \quad \delta_M > \frac{a_B\beta_{BM}\delta_B}{2\mu_B};$$
$$C_{12} : \lambda_M = \frac{\delta_M(\delta_M+\gamma_M)(2\mu_B(\gamma_B(\delta_B+\nu_B)+\delta_B(\delta_B+\mu_B+\nu_B))\delta_M - a_B\beta_{BM}\delta_B K)}{a_B^2\beta_{BM}\beta_{MB}\gamma_M\delta_B(\gamma_B+\delta_B)(\delta_B+\mu_B+\nu_B)}, \quad \delta_M > 0.$$

Now we have $\Delta = a_1^2 - 4a_2a_0 = d_0 + d_1\lambda_M + d_2\lambda_M^2$, where

$$\begin{aligned} d_0 &= a_B^2\beta_{BM}^2\delta_B^2\lambda_B^2(\gamma_B + \delta_B)(\delta_B + \mu_B + \nu_B)(\delta_M + \gamma_M)^2\delta_M^2 > 0, \\ d_1 &= 2a_B^2\beta_{BM}\beta_{MB}\gamma_M\delta_B\lambda_B(2\gamma_B\mu_B(\mu_B\delta_M - a_B\beta_{BM}\delta_B) \\ &\quad +(\gamma_B + \delta_B)(\delta_B + \mu_B + \nu_B)(a_B\beta_{BM}\delta_B - 2\mu_B\delta_M))\delta_M(\delta_M + \gamma_M), \\ d_2 &= a_B^4\beta_{BM}^2\beta_{MB}^2\gamma_M^2\delta_B^2(\gamma_B + \delta_B)(\delta_B + \mu_B + \nu_B) > 0. \end{aligned} \tag{13}$$

We can easily check that $d_1 - 4d_0d_2 \geq 0$ when $\delta_M \geq \frac{a_B\beta_{BM}\delta_B}{\mu_B}$. So two more curves can be defined by solving $\Delta = 0$, that is,

$$C_{upper} : \lambda_M = \frac{-d_1 + \sqrt{d_1^2 - 4d_0d_2}}{2d_2}, \quad \delta_M \geq \frac{a_B\beta_{BM}\delta_B}{\mu_B};$$
$$C_{lower} : \lambda_M = \frac{-d_1 - \sqrt{d_1^2 - 4d_0d_2}}{2d_2}, \quad \delta_M \geq \frac{a_B\beta_{BM}\delta_B}{\mu_B}.$$

We can also verify that C_1, C_{12}, C_{upper} and C_{lower} intersect at the point

$$P_1 = (\frac{a_B\beta_{BM}\delta_B}{\mu_B}, \frac{\beta_{BM}\delta_B\lambda_B(a_B\beta_{BM}\delta_B + \gamma_M\mu_B)}{\beta_{MB}\gamma_M\mu_B^2}).$$

At P_1, we can see that $a_2 = a_1 = 0$ and $\mathcal{R}_0 < 1$. Then there does not exist any solution for (7).

When $K \geq 0$ and $\delta_M > \frac{a_B\beta_{BM}\delta_B}{\mu_B}$, these five curves do not have any intersection. Moreover, C_{upper} is always above C_1. This implies that system (6) does not have multiple endemic equilibria (see Fig. 2(b)). When $K < 0$ and $\delta_M > \frac{a_B\beta_{BM}\delta_B}{\mu_B}$, we can verify that C_1, C_0 and C_{upper} intersect each other at P_2, where the horizontal coordinate of P_2 is $\frac{a_B\beta_{BM}\gamma_B\delta_B}{-K}$. In addition, the curve C_1 is above the other two curves where C_0 is above curve C_{upper}. Thus, in the region formed by C_0 and C_{upper} system (6) has two positive equilibria (see Fig. 2(a)).

Theorem 3.3. *If $\delta_M < \frac{a_B\beta_{BM}\gamma_B\delta_B}{(\delta_B+\gamma_B)(\delta_B+\mu_B+\nu_B)}$, then system (6) exhibits a backward bifurcation when $\mathcal{R}_0 = 1$. If $\beta_M < \frac{a_B\beta_{BM}\gamma_B\delta_B}{(\delta_B+\gamma_B)(\delta_B+\mu_B+\nu_B)}$, then the model exhibits a forward bifurcation when $\mathcal{R}_0 = 1$.*

Proof. Let $S_M = x_1$, $E_M = x_2$, $I_M = x_3$, $S_B = x_4$, $E_B = x_5$, $I_B = x_6$, $R_B = x_7$ and we denote $\lambda_M^* = \frac{\lambda_B(\delta_B+\gamma_B)(\delta_B+\mu_B+\nu_B)}{a_B^2\beta_{BM}\beta_{MB}\gamma_B\gamma_M\delta_B}\delta_M^2(\delta_M + \gamma_M)$. Then system (6) can be written as $\frac{df}{dt} = f(x, \phi)$ with $\phi = \lambda_M - \lambda_M^*$:

$$\begin{aligned} \frac{dx_1}{dt} &= \phi + \lambda_M^* - a_B\beta_{BM}\frac{x_1x_6}{x_4 + x_5 + x_6 + x_7} - \delta_M x_1 \\ \frac{dx_2}{dt} &= a_B\beta_{BM}\frac{x_1x_6}{x_4 + x_5 + x_6 + x_7} - \delta_M x_2 - \gamma_M x_2 \\ \frac{dx_3}{dt} &= \gamma_M x_2 - \delta_M x_3 \end{aligned}$$

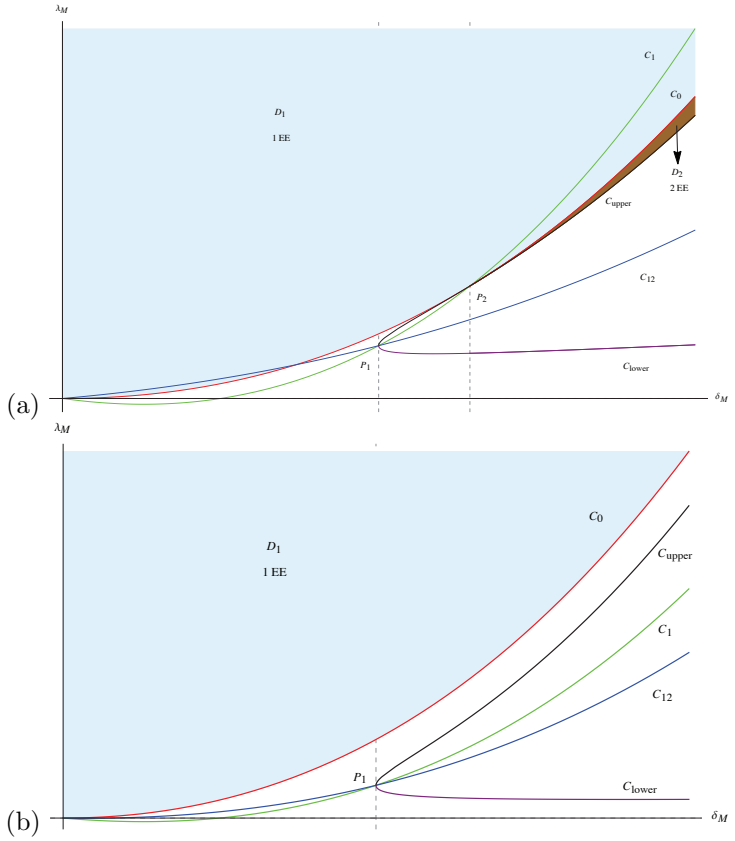

FIGURE 2. (a) When $\gamma_B(\delta_B - \mu_B + \nu_B) + \delta_B(\delta_B + \mu_B + \nu_B) < 0$, the bifurcation occurs on C_{upper}. (b) When $\gamma_B(\delta_B - \mu_B + \nu_B) + \delta_B(\delta_B + \mu_B + \nu_B) \geq 0$, system (6) has a unique endemic equilibrium if $\mathcal{R}_0 > 1$ and does not have any endemic equilibrium if $\mathcal{R}_0 < 1$.

$$\begin{aligned}
\frac{dx_4}{dt} &= \lambda_B - a_B\beta_{MB}\frac{x_3x_4}{x_4+x_5+x_6+x_7} - \delta_B x_4\\
\frac{dx_5}{dt} &= a_B\beta_{MB}\frac{x_3x_4}{x_4+x_5+x_6+x_7} - \delta_B x_5 - \gamma_B x_5\\
\frac{dx_6}{dt} &= \gamma_B x_5 - \delta_B x_6 - \mu_B x_6 - \nu_B x_6\\
\frac{dx_7}{dt} &= \nu_B x_6 - \delta_B x_7.
\end{aligned} \tag{14}$$

The Jacobian matrix at the disease-free equilibrium E_0 is

$$J(E_0) = \begin{pmatrix}
-\delta_M & 0 & 0 & 0 & 0 & -\frac{a_B\beta_B M(\phi+\lambda_M^*)\delta_B}{\delta_M\lambda_B} & 0\\
0 & -(\delta_M+\gamma_M) & 0 & 0 & 0 & \frac{a_B\beta_B M(\phi+\lambda_M^*)\delta_B}{\delta_M\lambda_B} & 0\\
0 & \gamma_M & \delta_M & 0 & 0 & 0 & 0\\
0 & 0 & a_B\beta_M B & 0 & -(\delta_B+\gamma_B) & 0 & 0\\
0 & 0 & 0 & 0 & \gamma_B & -(\delta_B+\mu_B+\nu_B) & 0\\
0 & 0 & 0 & 0 & 0 & \nu_B & \delta_B
\end{pmatrix}.$$

Denote $K_1 = \delta_M + \gamma_M$, $K_2 = \delta_B + \gamma_B$ and $K_3 = \delta_B + \mu_B + \nu_B$. When $\phi = 0$, the characteristic equation is

$$(\lambda + \delta_B)^2(\lambda + \delta_M)[(\lambda + \delta_M)(\lambda + K_1)(\lambda + K_2)(\lambda + K_3) - \delta_M K_1 K_2 K_3] = 0. \quad (15)$$

Then $\lambda = 0$ is a simple zero eigenvalue and all other eigenvalues have negative real part. Therefore, we can use the center manifold theory to discuss the bifurcation in this model.

First, $\phi = 0$ is equivalent to $\mathcal{R}_0 = 1$. When $\phi = 0$, the disease-free equilibrium E_0 is a nonhyperbolic equilibrium. Denote the left and right eigenvectors associated with the zero eigenvalue as ω and ν, respectively, here $\omega = (\omega_1, \omega_2, \omega_3, \omega_4, \omega_5, \omega_6, \omega_7)^T$ and $\nu = (\nu_1, \nu_2, \nu_3, \nu_4, \nu_5, \nu_6, \nu_7)$. Then they satisfy the following equations:

$$J(E_0)\omega = \nu J(E_0) = 0 \text{ and } \nu\omega = 1.$$

Thus, we have

$$\omega_1 = -\frac{K_1K_2K_3\delta_B}{a_B\beta_{MB}\nu_B\gamma_B\gamma_M},\ \omega_2 = \frac{K_2K_3\delta_B\delta_M}{a_B\beta_{MB}\nu_B\gamma_B\gamma_M},\ \omega_3 = \frac{K_2K_3\delta_B}{a_B\beta_{MB}\nu_B\gamma_B},$$
$$\omega_4 = -\frac{K_2K_3}{\nu_B\gamma_B},\ \omega_5 = \frac{K_3\gamma_B}{\nu_B\gamma_B},\ \omega_6 = \frac{\delta_B}{\nu_B},\ \omega_7 = 1.$$

and

$$\nu_1 = 0,\ \nu_2 = \frac{a_B\beta_{MB}\gamma_B\gamma_M}{K_1K_2\delta_M}\nu_6,\ \nu_3 = \frac{a_B\beta_M B\gamma_B}{K_2\delta_M}\nu_6,\ \nu_4 = 0,\ \nu_5 = \frac{\gamma_B}{K_2}\nu_6,$$
$$\nu_6 = \frac{K_1K_2\nu_B\delta_M}{\delta_B(K_1K_2K_3 + (K_1K_2 + K_2K_3 + K_1K_3)\delta_M)},\ \nu_7 = 0.$$

Now let $f_k(x, \phi)$ denote the k-th component of $f(x, \phi)$. Following the results given in Castillo-Chavez and Song [11], the bifurcation at $\phi = 0$ is backward when $a > 0$ and $b > 0$ and forward when $a < 0$ and $b > 0$, where a and b are defined as follows

$$a = \sum_{k,i,j=1}^{n} \nu_k\omega_i\omega_j \frac{\partial^2 f_k}{\partial x_i \partial x_j}(E_0, 0),$$
$$b = \sum_{k,i=1}^{n} \nu_k\omega_i \frac{\partial^2 f_k}{\partial x_i \partial \phi}(E_0, 0).$$

In this model

$$a = \frac{2\delta_B^2 K_3}{\lambda_B\nu_B^2\delta_M\gamma_B}(a_B\beta_{BM}\gamma_B\delta_B - K_2K_3\delta_M),$$
$$b = \frac{K_3}{\nu_B\lambda_M^*} > 0.$$

Thus, model (6) undergoes a backward bifurcation if $\delta_M < \frac{a_B\beta_{BM}\gamma_B\delta_B}{(\delta_B+\gamma_B)(\delta_B+\mu_B+\nu_B)}$ (i.e., a is positive) and a forward bifurcation if $\delta_M > \frac{a_B\beta_{BM}\gamma_B\delta_B}{(\delta_B+\gamma_B)(\delta_B+\mu_B+\nu_B)}$ (i.e., a is negative). □

According to the abover analysis, we can see that $\mathcal{R}_0 < 1$ cannot guarantee the global stability of the disease-free equilibrium due to the existence of the possible endemic equilibrium. The existence of backward bifurcation indicates that the disease now cannot be eradicated by simply reducing the basic reproduction number to be less than unity. Therefore, it is important to study backward bifurcation in epidemic models since it may provide some qualitative implications to disease control.

4. **Numerical simulations and applications to New York, Florida, Texas, and California.** In this section, we use our model to simulate the reported annual WNV human data provided by CDC. Considering that mosquitoes and birds only move in certain areas or along certain routes, we choose to study the WNV data of individual states instead of the whole U.S. The first case of human beings that has been identified in the U.S. was in New York City in 1999 and more cases have been reported continuously since then. So we will try to use our model to simulate the data from New York first. All parameter values for the four states are given in Table 2. To estimate some parameters such as the disease-related death rate, we summariez the WNV induced annaul death rates reported by CDC [7] for these four states in Tables 3.

TABLE 2. Parameter values used in the simulations for New York, Florida, Texas and California

Parameter	New York	Florida	Texas	California
λ_B	$48.4114 \times 10^5/yr$	$27.6550 \times 10^5/yr$	$28.4857 \times 10^5/yr$	$31.5153 \times 10^5/yr$
λ_M	$69.8528 \times 10^8/yr$	$16.3698 \times 10^8/yr$	$89.1128 \times 10^8/yr$	$61.9998 \times 10^8/yr$
λ_H	$4.03 \times 10^5/yr$	$3.47 \times 10^5/yr$	$4.6 \times 10^5/yr$	$7.54 \times 10^5/yr$
δ_B	$\frac{1}{8}/yr$	$\frac{1}{8}/yr$	$\frac{1}{8}/yr$	$\frac{1}{8}/yr$
δ_M	$8.9665/yr$	$8.0133/yr$	$7.5214/yr$	$9.4477/yr$
δ_H	$\frac{1}{78}/yr$	$\frac{1}{78}/yr$	$\frac{1}{78}/yr$	$\frac{1}{78}/yr$
γ_B	$9.90\%/yr$	$10.02\%/yr$	$10.20\%/yr$	$8.64\%/yr$
γ_M	$12.62\%/yr$	$12.79\%/yr$	$14.50\%/yr$	$17.41\%/yr$
γ_H	$20.00\%/yr$	$20.00\%/yr$	$20.00\%/yr$	$20.00\%/yr$
μ_B	$10.03\%/yr$	$13.93\%/yr$	$25.70\%/yr$	$12.26\%/yr$
μ_H	$8.50\%/yr$	$5.87\%/yr$	$5.36\%/yr$	3.62%/yr
ν_B	$12.25\%/yr$	$12.86\%/yr$	$13.25\%/yr$	$10.08\%/yr$
ν_H	$31.38\%/yr$	$39.89\%/yr$	$25.01\%/yr$	$35.65\%/yr$
a_B	$0.1532/day$	$0.1454/day$	$0.1589/day$	$0.1519/day$
a_H	$0.0552/day$	$0.0598/day$	$0.0726/day$	$0.0786/day$
β_{BM}	0.1600	0.1600	0.1600	0.1600
β_{MB}	0.8800	0.8800	0.8800	0.8800
β_{MH}	0.4023	0.2689	0.3525	0.2341

Numerical simulations of the infectious population and the number of accumulative deaths in New York are shown in Fig. 3. First we fixed the natural death rates of humans and birds as $\delta_H = \frac{1}{78}$ and $\delta_B = \frac{1}{8}$, respectively, from the assumption that the average life lengths of humans and birds are 78 years and 8 years, respectively. Also we fixed λ_H and $S_H(0)$ in New York according to the data from the United States Census Bureau [37]. γ_H is fixed at 0.2 since approximately only 20% of exposed individuals becomes infectious. We also fixed γ_B, β_{BM} and β_{MB} according to Wonham et al. [40]. The initial values about $I_M(0)$, $I_B(0)$, and $I_H(0)$ were decided by the reported data in New York in 2000. After we assumed $R_H(0) = 0$, other initial values were regarded as parameters. In order to determine the parameter values that can be used to fit the data, now we try to minimize

$$Chi2 = \sum \left(\frac{(Data - Simulation)^2}{Simulation} + \frac{(Death - Simulation)^2}{Simulation} \right).$$

All the unknown parameters were estimated by the MATLAB tool fminsearch and the results are shown in Table 2. In Table 1 the values or the value ranges of some parameters are given. Firstly, we use the data from New York to obtain

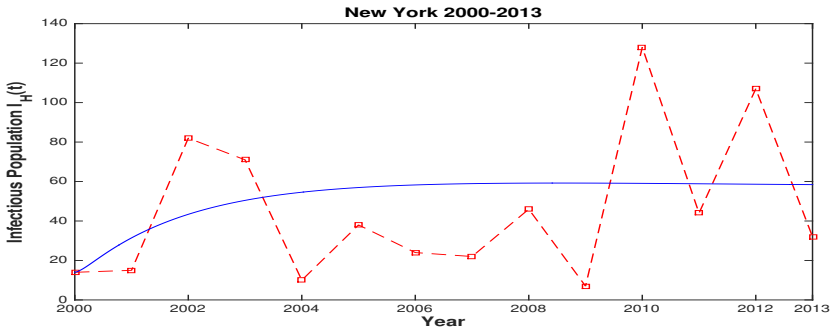

(a)

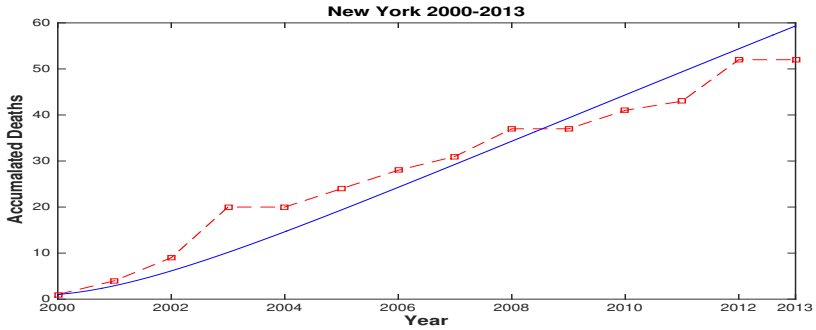

(b)

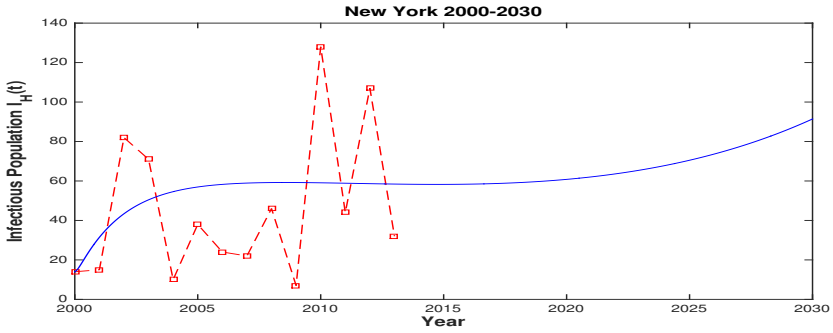

(c)

FIGURE 3. Comparisons of the reported human WNV cases from CDC (dashed curve) and the solution of the infected human population $I_h(t)$ (solid curve) of our model (1): (a) Simulation of the reported human WNV data for New York from 2000-2013; (b) Simulation of the accumulative deaths from New York from 2000-2013; (c) Prediction of human WNV cases from New York from 2000-2030.

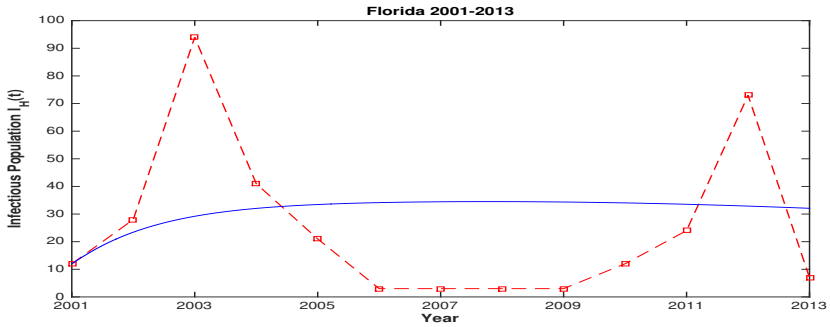

(a)

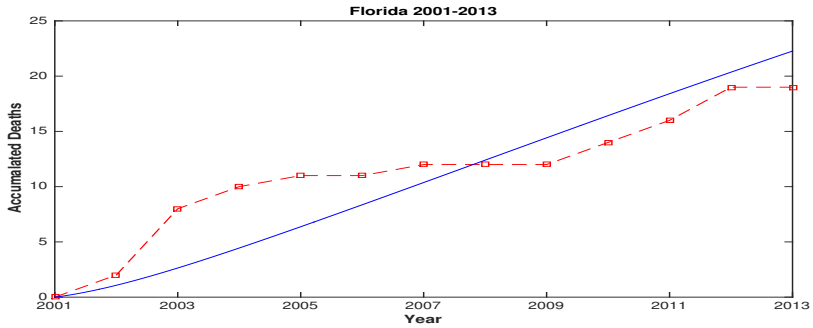

(b)

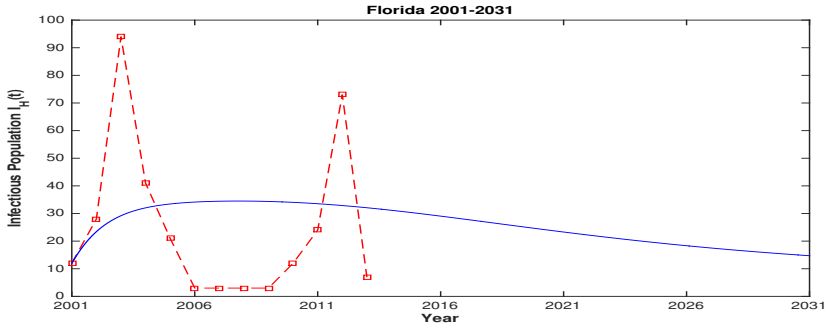

(c)

FIGURE 4. Comparisons of the reported human WNV cases from CDC (dashed curve) and the solution of the infected human population $I_h(t)$ (solid curve) of our model (1): (a) Simulation of the reported human WNV data for Florida from 2001-2013; (b) Simulation of the accumulative deaths from Florida from 2001-2013; (c) Prediction of human WNV cases from Florida from 2001-2031.

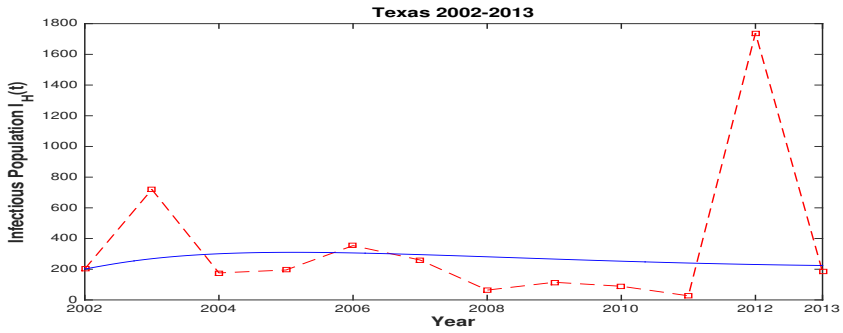

(a)

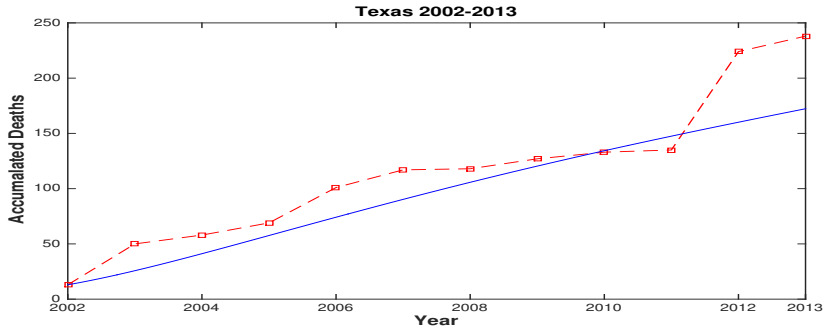

(b)

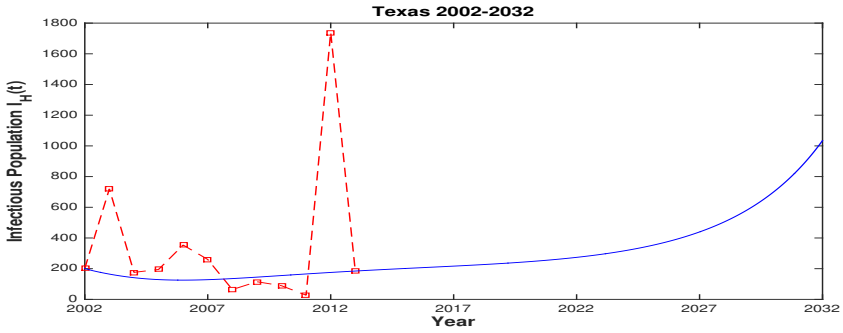

(c)

FIGURE 5. Comparisons of the reported human WNV cases from CDC (dashed curve) and the solution of the infected human population $I_h(t)$ (solid curve) of our model (1): (a) Simulation of the reported human WNV data for Texas from 2002-2013; (b) Simulation of the accumulative deaths from Texas from 2002-2013; (c) Prediction of human WNV cases from Texas from 2002-2032.

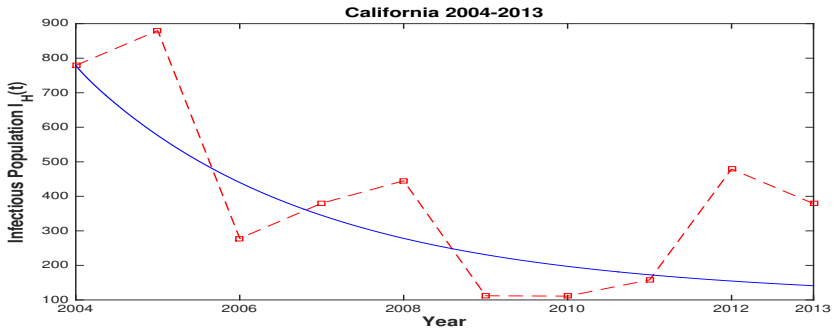

(a)

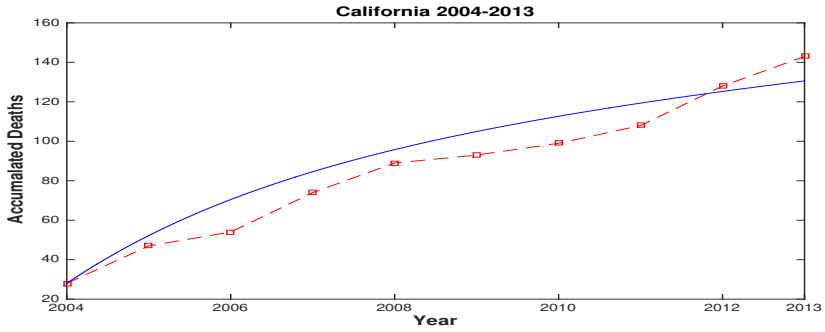

(b)

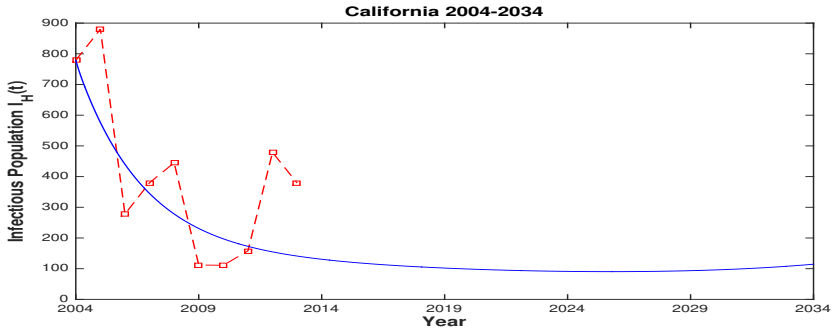

(c)

FIGURE 6. Comparisons of the reported human WNV cases from CDC (dashed curve) and the solution of the infected human population $I_h(t)$ (solid curve) of our model (1): (a) Simulation of the reported human WNV data for California from 2004-2013; (b) Simulation of the accumulative deaths from California from 2004-2013; (c) Prediction of human WNV cases from California from 2004-2034.

TABLE 3. WNV induced annually death rates in New York, Florida, Texas and California from 1999 to 2013 (CDC [7])

	New York	Florida	Texas	California
1999	11%	NA	NA	NA
2000	7%	NA	NA	NA
2001	2%	0%	NA	NA
2002	6%	7%	6%	0%
2003	15%	6%	5%	0%
2004	0%	5%	5%	4%
2005	11%	5%	6%	2%
2006	17%	0%	9%	3%
2007	14%	33%	6%	5%
2008	13%	0%	2%	3%
2009	0%	0%	8%	4%
2010	7%	17%	3%	5%
2011	5%	8%	7%	6%
2012	8%	4%	5%	4%
2013	0%	0%	8%	4%
Average	8.50%	5.87%	5.36%	3.62%

a set of baseline parameter values. Using these parameter values, we carry out numerical simulations of our model and obtain a reasonable match between the solution of the infectious population $I_H(t)$ of our model (1) and the WNV human data from CDC in New York from 2000 to 2013 in Fig. 3 (a). Moreover, the simulated number of accumulative deaths fits the data well in Fig. 3 (b). There was an overestimation from 2004 to 2009 in Fig. 3 (a). As a matter of fact, WNV caused the largest outbreak of neuroinvasive disease ever recorded in the Western Hemisphere, with 9,862 cases reported overall, including 264 deaths in 2002 (Bajwa et al. [2]). New York began to focus on the control of mosquito population in 2003 and measures taken by New York City Department of Health and Mental Hygiene indeed substantially controlled the spread of the disease in the next 5 years. However, the simulation result in Fig. 3 (c) indicates that the current prevention and control strategies cannot guarantee the eradication of the disease and also presents the evidence for the increase in the number of infected WNV human cases in the next 30 years.

Next, based on the baseline parameter values from New York, we adjust some parameters accordingly (within their value ranges) in order to fit the data from Florida, Texas, and California. In Fig. 4 -6, similar results can be observed: the system of WNV has not reached its equilibrium yet in the states of New York, Texas, and California and the disease could not be eradicated in these three states under current prevent and control strategies. Therefore, the WNV disease in the U.S. has not reached its equilibrium yet and there may be more sporadic and large WNV outbreaks in the future if the current control and prevention strategies are not enhanced. These simulation results suggest the need for seeking more effective and useful control measures for the outbreaks of WNV in the U.S.

Note that some parameter values are the same for all four states, while some other parameter vlaues are chosen differently for different states in order to provide

better fits for each data set. In fact, as CDC reported, the incidence rates and the disease-related death rates for these states are different (see CDC [7] and Table 3). These could be interpreted as that the four states have different geograph locations, different climate changes, different environmental conditions, etc.

Numerical simulations were also carried out with a variety of initial conditions to investigate the influence of the initial population sizes on the infectious population $I_H(t)$. It is found that the infection is more sensitive to the size of susceptible mosquito population than to other initial conditions. Fig. 7 shows that the increase in the mosquito population will lead to the increase of the number of infected human cases. This suggests that reducing the population size of mosquitoes is a useful method to control the prevalence of the disease.

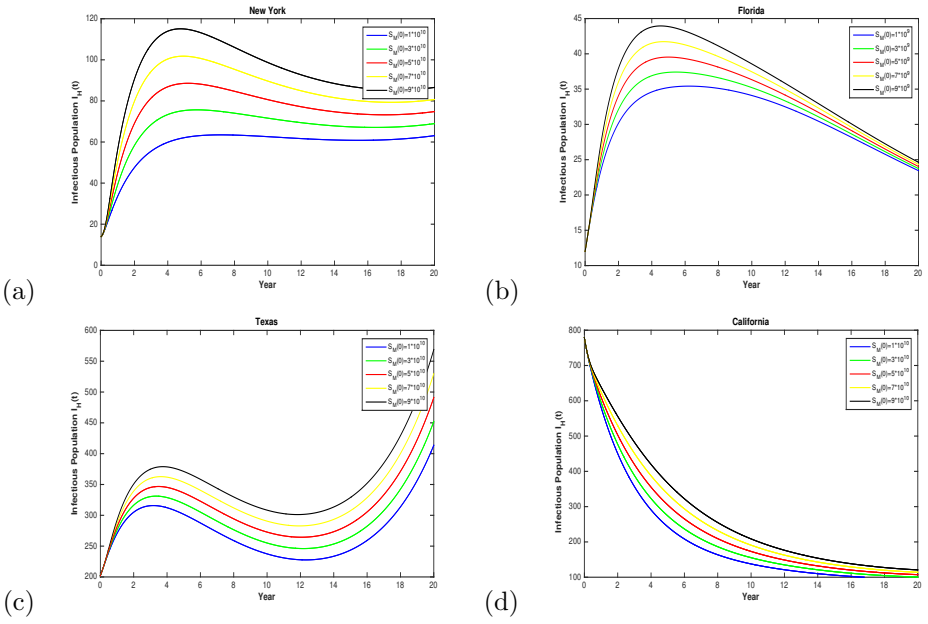

FIGURE 7. Effects of the initial mosquito population size $S_M(0)$ on the number of infected humans $I_H(t)$ in (a) New York, (b) Florida, (c) Texas, and (d) California.

To provide some effective control measures about mosquitoes, we also perform some sensitivity analyses of the basic reproduction number $\mathcal{R}_0$ in terms of other parameters. Under current parameter values, the basic reproduction number in New York is $\mathcal{R}_0^{\mathrm{NY}} = 1.3742$ and the disease will not be eradicated. Also, $\mathcal{R}_0^{\mathrm{FL}} = 0.9390$, $\mathcal{R}_0^{\mathrm{TX}} = 2.4245$, and $\mathcal{R}_0^{\mathrm{CA}} = 1.6616$. Fig. 8 reflects three important factors to control the disease: the death rate of mosquitoes δ_M, the recruitment rate of mosquitoes λ_M, and the biting rate of mosquitoes on birds a_B. Obviously the biting rate of mosquitoes on birds can be reduced if the population size of mosquitoes decreases significantly. For instance, to reduce the basic reproduction number below than 1 in New York, we should at least decrease the recruitment rate of mosquitoes by 50% or increase the death rate of mosquitoes by 25% from the current level. In Texas, which has a larger basic reproduction number, these two numbers need to be larger than that in New York.

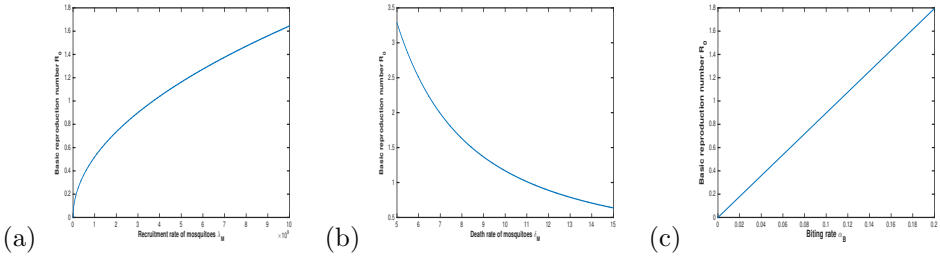

FIGURE 8. The basic reproduction number R_0 in terms of (a) recruitment rate of mosquitoes λ_M, (b) death rate of mosquitoes δ_M, and (c) the biting rate of mosquitoes on birds a_B in New York.

It is possible to achieve a sufficiently small basic reproduction number by controlling either λ_M or δ_M in New York. Fig. 9 (a) provides the evidence that neither of these two factors by itself plays a dominant role in controlling the disease. However the situation in Texas is different. According to Fig. 9(c), it is almost impossible to eliminate the disease in Texas by only reducing the recruitment rate of mosquitoes λ_M. Meanwhile, the death rate of mosquitoes δ_M plays a more important role here, therefore a combination of these two methods is more efficient in Texas. In fact, numerous measures including the aerial spraying of adulticide were taken in Texas to control the outbreak of WNV in 2012. Thus the basic reproduction number now is believed to be smaller than the one estimated by us.

A more precise and direct comparison is given to investigate their effects on the disease (see Fig. 10). We achieve the same basic reproduction number by decreasing the recruitment rate of mosquitoes λ_M or increasing the death rate of mosquitoes δ_M in New York. The effects of these two are almost the same in a long term observation. However, the second method can reduce the size of the infectious population immediately.

A smaller recruitment rate of mosquitoes is always accomplished by the larval mosquito control plan and water management. Meanwhile a larger death rate of mosquitoes usually depends on the adult mosquito control plan. Actually larval mosquito control is preferred to the adult mosquito control if some realistic factors are taken into consideration. It is believed that larviciding is one of the most effective and ecologically safe methods to control the West Nile virus while the adulticiding may cause concerns as to its environmental effect, the influence on the non-target insects and the strictly controlled volume. The observation from our simulations shows that the first method which leads to the reduction of the recruitment rate of mosquitoes is able to help disease control. However, this is not always enough to eliminate the disease. In this case, the adulticiding is more efficient and effective. This indicates that adulticiding can be applied as a control strategy when the surveillance data indicates a high risk of disease outbreaks. We should emphasize that while a larval mosquito control strategy cannot guarantee the elimination of the disease it still plays a significant role in the long term disease control.

5. **Discussion.** Since the outbreak of WNV in New York City in 1999, great attention has been paid to studying the biological, ecological, epidemiological, and medical characters of the virus and many interesting mathematical models have

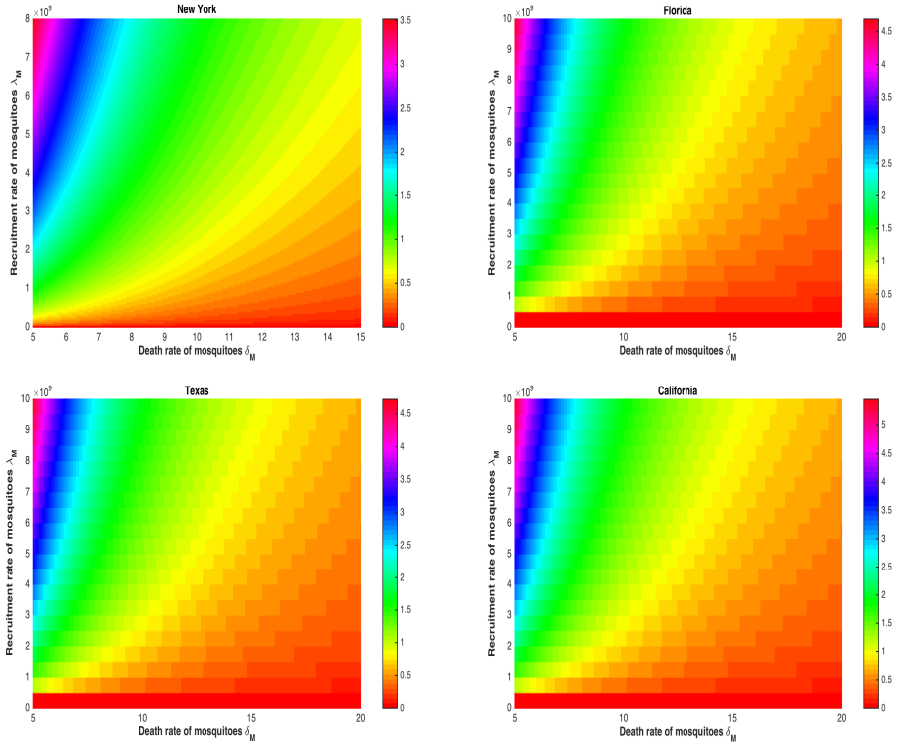

FIGURE 9. The basic reproduction number R_0 in terms of the recruitment rate λ_M and the death rate δ_M of mosquitoes for New York, Florida, Texas, and California.

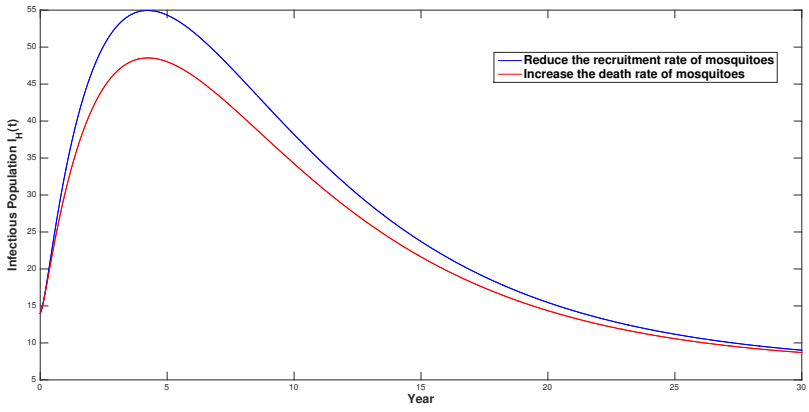

FIGURE 10. Comparison of the effects of decreasing the recruitment rate of mosquitoes λ_M and increasing the death rate of mosquitoes δ_M in New York from 2000.

also been developed to investigate the transmission dynamics of the diseases, see Thomas & Urena [36], Wonham et al. [40], Cruz-Pacheco et al. [12], Bowman et al. [4], Laperriere et al. [22], Wan and Zhu [39], Simpson et al. [34], the survey by Wonham et al. [41] and the references cited therein. Most of these models focus on the interaction between birds and mosquitoes. Humans are regarded as dead-end host since infected humans do not spread the virus further to any species. Thus it is reasonable to include only the transmission of the virus between birds and mosquitos in order to understand the transmission dynamics of WNV among these two species. However, from both public health and epidemiology points of view, it is necessary to include the human component in the models: First, WNV is an emerging mosquito-borne RNA virus which has caused significant illness and death worldwide, including the U.S.. In the absence of a specific treatment and vaccine of WNV, further research is needed to understand the epidemiology and pathology of WNV. Second, most existing WNV data are on reported human cases (in particular the human WNV data from the U.S. reported by the CDC) which have hardly been simulated in the literature. Using more comprehensive models including birds, mosquitoes and humans to simulate the human data will certainly help validating the models and will provide better understanding the transmission dynamics of the disease among all three species. Third, we believe that considering the mosquito population dynamics will help to design more effective and environmental friendly mosquito control measures for reducing human WNV infected cases.

For these purposes, we have proposed a deterministic model to describe the transmission of WNV between birds, mosquitoes, and humans and studied its dynamical behavior. By estimating the parameter values, we used the model to simulate the human WNV data from the states of New York, Florida, Texas, and California as reported to the CDC and predict the spread of the disease in these states for the next 20 years or so. We believe that it is the first time the human WNV data from these states have been systematically simulated by using mathematical models. These numerical simulations indicate that the WNV disease has not reached its equilibrium yet in most states (and thus in the U.S.) and it may get worse if the current control and prevention strategies are not enhanced.

In order to seek for effective control measures to prevent outbreaks of WNV in the U.S., we performed various numerical simulations of the model. Figure 7 showed the effect of the initial susceptible mosquito population size $S_M(0)$ on the level of the infectious human population $I_H(t)$ for all four states, which demonstrated that reducing the mosquito population size is a useful method to control the prevalence of the diseases in humans, and thus further confirmed that mosquito control is one of the main WNV prevention strategies (Bowman et al. [4]).

Since mosquito control could be classified further as larval mosquito control and adult mosquito control, next we would like to know which of these control measures is more effective and how such specific mosquito control measures affect the prevalence of the disease at the human level. As shown in Fig. 8 and Fig. 9, we performed sensitivity analyses of the basic reproduction number in terms of the recruitment (birth) rate of mosquitoes λ_M, the death rate of mosquitoes δ_M, and the biting rate of mosquitoes on birds a_B for New York. Notice that the biting rate of mosquitoes on birds can be reduced if the mosquito population size decreases. Thus, these sensitivity analyses indicate that the essential purpose of the control strategies should be to increase the death rate and decrease the recruitment (birth)

rate of mosquitoes. In fact, both of these two strategies play essential roles in reducing the infectious population and controlling the disease (Fig. 9). Usually the increase of the death rate of mosquitoes, which is mostly accomplished by adulticiding (killing adult mosquitoes), works immediately to control the disease. Clearly the reduction of the recruitment (birth) rate of mosquitoes leads to a reduction of the infectious human population (Fig. 7 and Fig. 9). Considering together with the practical application, this suggests using larviciding (killing mosquito larvae) as the primary measure, while adulticiding should be performed as an emergency method if the surveillance data indicates a significant risk. Indeed, the outbreak of WNV in Texas in 2012 caused 89 deaths and 1868 reported cases. Dallas County, one of the most severe areas, used aerial spraying of adulticide to curb the mosquito population. However, local residents were concerned with the health effects of such a spraying to humans and other animals. The larval mosquito control mainly focuses on the source reduction, which can range from draining roadside ditches to properly disposing the discarded tires (CDC [6]), and on larviciding, which include biological larvicides and chemistry larvicides. Most of these methods we mentioned here will not do any harm to the environment.

In conclusion, a combination of the larval and adult mosquito control is important and effective for controlling the disease and preventing large local outbreaks. The larval mosquito control should be taken as early as possible in a season to control the mosquito population size and the adult mosquito control measure is necessary for immediately preventing the transmission of WNV from mosquitoes to birds and humans.

WNV is a complex of distinct human pathogens, different mosquito species can transmit the virus and various avian species play roles as reservoir species. Seasonality certainly plays a crucial role in affecting the population dynamics of mosquitoes and birds and thus the transmission dynamics of WNV. The data from CDC also exhibit periodic (seasonal) patterns. Therefore, it will be very important and interesting to study the effect of seasonal and climatic change on the spread of WNV. It should be pointed out that the time unit for our current model and numerical simulations is a year since we used the reported annual WNV human data. If seasonal effect is included in the model, then the time unit has to be changed to a month and, correspondingly, monthly WNV data are needed. Twelve month periodic functions can be used to describe the infection rates (see, for example, Zhang et al. [43]), and the periodic model can be used to describe the seasonal outbreaks of WNV and to simulate the monthly data on human WNV cases in the U.S. Moreover, spatial and host heterogeneities are important factors as well since some birds are local nonmigratory peridomestic species while others are migratory and can carry infections over vast distances. Lewis et al. [23], Maidana & Yang [26] proposed reaction-diffusion models for the spatial spread of WNV in terms of traveling waves. See also Magori et al. [25]. Liu et al. [24] formulated a patch model to consider the geographical spread of WNV. Pybus et al. [31] demonstrated that the dispersal of WNV is greater and far more variable than previously measured, such that its dissemination was critically determined by rare, long-range movements that are unlikely to be discerned during field observations, and that genetic data can be used to measure the spatial dynamics of natural populations. We believe that one might employ a patch-network modeling framework (see Chen et al. [8]) to consider the impact of both migratory and nonmigratory reservoir avian species on WNV and

to simulate the case in some regions where the epidemic dies out and the epidemics in following years are caused by reintroductions.

REFERENCES

[1] J. F. Anderson, T. G. Andreadis, C. R. Vossbrinck, S. Tirrell, E. Wakem, A. Garmendia and H. J. Van Kruiningen, Isolation of West Nile virus from mosquitoes, crows, and a cooper's hawk in Connecticut, *Science*, **286** (1999), 2331–2333.

[2] W. Bajwa, M. O'Connor, B. E. Slavinski and Z. Shah, *Comprehensive Mosquito Surveillance and Control Plan 2012*, New York City Department of Health and Mental Hygiene, New York, 2012. Available from: http://www1.nyc.gov/assets/doh/downloads/pdf/wnv/wnvplan2012.pdf.

[3] C. G. Blackmore, L. M. Stark, W. C. Jeter, R. L. Oliveri, R. G. Brooks, L. A. Conti and S. T. Wiersma, Surveillance results from the first West Nile virus transmission season in Florida, 2001, *The American Journal of Tropical Medicine and Hygiene*, **69** (2003), 141–150.

[4] C. Bowman, A. B. Gumel, P. van den Driessche, J. Wu and H. Zhu, A mathematical model for assessing control strategies against West Nile virus, *Bulletin of Mathematical Biology*, **67** (2005), 1107–1133.

[5] T. Briese, X. Y. Jia, C. Huang, L. J. Grady and W. I. Lipkin, Identification of a Kunjin/West Nile like flavivirus in brains of patients with New York encephalitis, *Lancet*, **354** (1999), 1261–1262.

[6] Centers for Disease Control and Prevention (CDC), *West Nile Virus in the United States: Guidelines for Surveillance, Prevention, and Control*, June 4, 2013. Available from: http://www.cdc.gov/westnile/resources/pdfs/wnvGuidelines.pdf.

[7] Centers for Disease Control and Prevention (CDC), *West Nile Virus*, March 26, 2014. Available from: http://www.cdc.gov/westnile/index.html.

[8] J. Chen, L. Zou, Z. Jin and S. Ruan, Modeling the geographic spread of rabies in China, *PLoS Neglected Tropical Diseases*, **9** (2015), e0003772.

[9] T. M. Colpitts, M. J. Conway, R. R. Montgomery and E. Fikrig, West Nile Virus: Biology, transmission, and human infection, *Clinical Microbiology Reviews*, **25** (2012), 635–648.

[10] R. B. Clapp, M. K. Klimkiewicz and A. G. Futcher, Longevity records of North American birds: Columbidae through paridae, *Journal of Field Ornithology*, **54** (1983) (2), 123–137.

[11] C. Castillo-Chavez and B. Song, Dynamical models of Tuberculosis and their applications, *Mathematical Biosciences and Engineering* , **1** (2004), 361–404.

[12] G. Cruz-Pacheco, L. Esteva, J. A. Montaño-Hirose and C. Vargas, Modelling the dynamics of West Nile virus, *Bulletin of Mathematical Biology*, **67** (2005), 1157–1172.

[13] O. Diekmann, J. A. P. Heesterbeek and J. A. J. Metz, On the definition and the computation of the basic reproduction ratio R_0 in models for infectious diseases in heterogeneous populations, *Journal of Mathematical Biology*, **28** (1990), 365–382.

[14] O. Diekmann, J. A. P. Heesterbeek and M. G. Roberts, The construction of nextgeneration matrices for compartmental epidemic models, *Journal of the Royal Society Interface*, **7** (2009), rsif20090386.

[15] M. Eidson, L. Kramer, W. Stone, Y. Hagiwara, K. Schmit and New York State West Nile Virus Avian Surveillance Team, Dead bird surveillance as an early warning system for West Nile virus, *Emerging Infectious Diseases*, **7** (2001), 631–635.

[16] G. L. Hamer, U. D. Kitron, T. L. Goldberg, J. D. Brawn, S. R. Loss, M. O. Ruiz, D. B. Hayes and E. D. Walker, Host selection by Culex pipiens mosquitoes and West Nile virus amplification, *The American Journal of Tropical Medicine and Hygiene*, **80** (2009) (2), 268–278.

[17] C. G. Hayes, West Nile Virus, in *The Arboviruses: Epidemiology and Ecolog* (eds. T.P. Monath), CRC, Boca Raton, FL, 1989, pp. 59–88.

[18] E. B. Hayes and D. J. Gubler, West Nile Virus: Epidemiology and clinical features of an emerging epidemic in the United States, *Annual Review of Medicine*, **57** (2006), 181–194.

[19] A. M. Kilpatrick, P. Daszak, M. J. Jones, P. P. Marra and L. D. Kramer, Host heterogeneity dominates West Nile virus transmission, *Proceedings of the Royal Society of London B: Biological Sciences*, **273** (2006), 2327–2333.

[20] N. Komar, West Nile virus: Epidemiology and ecology in North America, *Advances in Virus Research*, **61** (2003), 185–234.

[21] R. S. Lacciotti, J. T. Roehrig, V. Deubel, J. Smith and M. Parker et al., Origin of the West Nile virus responsible for an outbreak of encephalitis in the northeastern United States, *Science*, **286** (1999), 2333–2337.

[22] V. Laperriere, K. Brugger and F. Rubel, Simulation of the seasonal cycles of bird, equine and human West Nile virus cases, *Preventive Veterinary Medicine*, **98** (2011), 99–110.

[23] M. A. Lewis, J. Renclawowicz and P. van den Driessche, Traveling waves and spread rates for a West Nile Virus model, *Bulletin of Mathematical Biology*, **68** (2006), 3–23.

[24] R. Liu, J. Shuai, J. Wu and H. Zhu, Modeling spatial spread of West Nile virus and impact of directional dispersal of birds, *Mathematical Biosciences and Engineering*, **3** (2006), 145–160.

[25] K. Magori, W. I. Bajwa, S. Bowden and J. M. Drake, Decelerating spread of West Nile Virus by percolation in a heterogeneous urban landscape, *PLoS Computational Biology*, **7** (2011), e1002104, 13pp.

[26] N. A. Maidana and H. M. Yang, Spatial spreading of West Nile Virus described by traveling wave, *Journal of Theoretical Biology*, **258** (2009), 403–417.

[27] A. A. Marfin and D. J. Gubler, West Nile encephalitis: An emerging disease in the United States, *Clinical Infectious Diseases*, **33** (2001), 1712–1719.

[28] K. O. Murray, E. Mertens and P. Després, West Nile virus and its emergence in the United States of America, *Veterinary Research*, **41** (2010), p67.

[29] M. S. Nolan, J. Schuermann and K. O. Murray, West Nile virus infection among humans, Texas, USA, 2002-2011, *Emerging Infectious Diseases*, **19** (2013), 137–139.

[30] D. R. O'Leary, A. A. Marfin, S. P. Montgomery, A. M. Kipp, J. A. Lehman, B. J. Biggerstaff, V. L. Elko, P. D. Collins, J. E. Jones and G. L. Campbell, The epidemic of West Nile virus in the United States, *Vector-Borne and Zoonotic Diseases*, **4** (2004), 61–70.

[31] O. G. Pybus, M. A. Suchard, P. Lemey, F. J. Bernardin, A. Rambaut, F. W. Crawford, R. R. Gray, N. Arinaminpathy, S. L. Stramer, M. P. Busch and E. L. Delwart, Unifying the spatial epidemiology and molecular evolution of emerging epidemics, *Proceedings of the National Academy of Sciences*, **109** (2012), 15066–15071.

[32] W. Reisen, H. Lothrop, R. Chiles, M. Madon, C. Cossen, L. Woods, S. Husted, V. Kramer and J. Edman, West nile virus in california, *Emerging Infectious Diseases*, **10** (2004), 1369–1378.

[33] F. Rubel, K. Brugger, M. Hantel, S. Chvala-Mannsberger, T. Bakonyi, H. Weissenbock and N. Nowotny, Explaining Usutu virus dynamics in Austria: Model development and calibration, *Preventive Veterinary Medicine*, **85** (2008), 166–186.

[34] J. E. Simpson, P. J. Hurtado, J. Medlock, G. Molaei, T. G. Andreadis, A. P. Galvani and M. A. Diuk-Wasser, Vector host-feeding preferences drive transmission of multi-host pathogens: West Nile virus as a model system, *Proceedings of the Royal Society of London B: Biological Sciences*, **279** (2008) (1730), 925–933.

[35] K. E. Steele, M. J. Linn, R. J. Schoepp, N. Komar, T. W. Geisbert, R. M. Manduca, P. R. Calle, B. L. Raphael, T. L. Clippinger, T. Larsen, J. Smith, R. S. Lanciotti, N. A. Panella and T. S. Mc Namara, Pathology of fatal West Nile virus infections in native and exotic birds during the 1999 outbreak in New York City, NY, *Veterinary Pathology*, **37** (2000), 208–224.

[36] D. M. Thomas and B. Urena, A model describing the evolution of West Nile-like encephalitis in New York City, *Mathematical and Computer Modelling*, **34** (2001), 771–781.

[37] *United States Census Bureau, 2013 Historical Population Data*, last updated Sept. 25, 2013. Available from: `http://www.census.gov/popest/data/historical/index.html`.

[38] P. van den Driessche and J. Watmough, Reproduction numbers and sub-threshold endemic equilibria for compartmental models of disease transmission, *Mathematical Biosciences*, **180** (2002), 29–48.

[39] H. Wan and H. Zhu, The backward bifurcation in compartmental models for West Nile virus, *Mathematical Biosciences*, **227** (2010), 20–28.

[40] M. J. Wonham, T. de Camino-Beck and M. A. Lewis, An epidemiological model for West Nile virus: Invasion analysis and control applications, *Proceedings of the Royal Society of London B: Biological Sciences*, **271** (2004), 501–507.

[41] M. J. Wonham, M. A. Lewis, J. Renclawowicz and P. van den Driessche, Transmission assumptions generate conflicting predictions in host-vector disease models: A case study in West Nile virus, *Ecology Letters*, **9** (2006), 706–725.

[42] *World Health Organization: West Nile virus*, 2015. Available from: http://www.who.int/mediacentre/factsheets/fs354/en/.

[43] J. Zhang, Z. Jin, G. Q. Sun, X. D. Sun and S. Ruan, Modeling seasonal rabies epidemic in China, *Bulletin of Mathematical Biology*, **74** (2012), 1226–1251.

Received April 2016; revised June 2016.

E-mail address: jchen@math.miami.edu
E-mail address: hjc@mail.ccnu.edu.cn
E-mail address: jbeier@med.miami.edu
E-mail address: rsc@math.miami.edu
E-mail address: gcc@math.miami.edu
E-mail address: dofuller@miami.edu
E-mail address: guoyan_zhang@doh.state.fl.us
E-mail address: ruan@math.miami.edu